PARALLEL MEASUREMENT OF COMPRESSIONAL AND SHEAR WAVES IN TRIAXIAL APPARATUS AT ISOTROPIC AND ANISOTROPIC STRESS STATES

Laxmi Prasad SUWAL[1] and Reiko KUWANO[2]

ABSTRACT: Flat piezo-ceramic element based Disk Transducer has been developed to investigate the material's properties propagating elastic waves on laboratory specimens. Extending its applicability, both compressional and shear waves were propagated on a single specimen simultaneously and signals were successfully acquired at same time. Second, elastic parameters, small strain stiffness and Poisson's ratios were evaluated based on the simultaneously acquired signals on cylindrical triaxial specimen on granular soils. Elastic properties of three sorts of granular materials, fine, medium coarse and coarse sands were investigated at isotropic and anisotropic stress states in laboratory. Axial and lateral strains were locally evaluated by Local Deformation Transducer (LDT) and clip gauges. Small strain stiffness and Poisson's ratios were directly evaluated employing small strain (≈0.001%) cyclic loadings in vertical direction. With simultaneously acquired compressional and shear waves, elastic parameters were indirectly determined in both isotropic and anisotropic stress states. Well interpretable waveforms were observed during parallel measurement of both the compressional and the shear waves. The static method applying small strain cyclic loadings and Disk Transducer method with parallel measurement of both the compressional and the shear waves showed well agreed results.

Key Words: Compressional wave, Shear wave, Young's modulus, Shear modulus, Wave measurement, Laboratory test, Granular material

INTRODUCTION

Elastic waves associated with the materials properties. The thoroughly studies of the propagated elastic waves are quite informative to investigate the soil properties and has been established as a good tool in field and laboratory based studies. Lawrence (1963, 1965) was probably the first to use the flat piezo-electric transducers in shear wave measurement in soil specimens. Bimorph element (piezo ceramic element) based transducer "Bender element" has gained the popularity amongst the researchers after its development by Shirley and Hampton (1977). Many researchers followed this development and extensively used with modifications as their requirements such as used in consolidometer or odometer (Jamiolkowski et at., 1995, Lee et al., 2010), triaxial apparatus (Viggiani and Atkinson, 1995; Jovicic et al., 1996), Shear apparatus (Mulmi, S., 2008) etc.

Stress-strain relationship is basic property of material. Many materials exhibit the linear relationship at initial very small strain level. In daily working loading perturbations, geo-materials experience only small strain less than 0.1% (Burland, 1989; Tatsouka and Kohata, 1995). Therefore, it is realized that elastic components are playing important role in deformation characteristics of geo-materials. A real elastic and linear behavior region of soil is very small (≤ 0.001%) and not easy to determine accurately due to the limitation of measurement technique. The linear, elastic and recoverable stress strain relationship were found up to 0.001% strain variation for most of soils. The stiffness modulus within elastic range of strain is known as the small strain stiffness modulus and it is being used in

[1] Graduate Student, Department of Civil Engineering, University of Tokyo
[2] Associate Professor, Institute of Industrial Science, University of Tokyo

analysis and design of geotechnical structures. This constant stiffness modulus reflects an identical property of various geo-materials and is equivalent to that derived by elastic wave measurement technique. The wave propagation techniques allow to perform reliable experiments to study the mechanical properties of materials in small strain range (Viggiani,and Atkinson, 1995; Brignoli et al., 1996; Kuwano et al., 1999). Precise local strain measurement is essential to evaluate elastic parameters; small strain stiffness and Poisson's ratio. Local strains are needed to be measured to minimize the effects of bedding errors and system compliance (Burland and Symes 1982, Goto et al. 1991, Tatsuoka and Shibuya 1992, Lo Presti et al. 1993, Tatsuoka and Kohata 1995). Several researchers have attempted to develop a reliable technique for measuring local strain. Inclinometers were developed at the Imperial College of London (Burland and Symes, 1982; Ackerly et al., 1987). Local Deformation Transducer (LDT) was invented at the University of Tokyo (Goto et al., 1991). Non-contact transducers and devices are also being used (Hird and Yung, 1989; Hicher, 1996; Di Benedetto et.al., 1997).

Recently a flat disk shaped piezo ceramic transducer, called Disk Transducer measuring both compressional and shear waves has been developed in the University of Tokyo (Suwal and Kuwano 2010). Exploring its applicability and ability, the attempt to measure simultaneously both the compressional and shear waves were done in this study. Elastic wave propagation through soil is usual and established. However, the acquisition of both the compressional and the shear waves in parallel are rare in geotechnical engineering sector. The efforts of propagating individual the compressional and the shear waves as well as simultaneously the compressional and the shear waves on granular soils including rubber dummy have successfully done and the equivalent result were found. In addition, elastic parameters; Young's moduli and Shear moduli were investigated by propagating the compressional and shear waves simultaneously on three kinds of granular soils at various stress state. Those parameters are statically evaluated applying small strain cyclic loading in same stress states and the achieved results were compared.

TRANSDUCER DESIGN AND LAYOUT IN APPARATUS

Piezoelectric effect is defined as the relation between mechanical distortion and an electrical voltage in solids. Industrially it is produced heating polycrystal under the application of strong electric field. In heated condition, molecules are able to move freely and electric field controls the polling axis to get well defined piezoelectric effect. The piezoelectric crystal vibrates in several ways at different frequencies. Ceramics are well suited materials to produce piezoelectric elements. Flat disk shaped piezo-elements consisting of a central core of polarized piezoelectric ceramic sandwiched between two thin electrodes at the top and bottom surfaces are employed in this study which is produced by "Lead Zicronate Titanate Ceramic [Pb(Ti.Zr)O3]".The nature of the vibration depends upon the direction of polarization. Figure 1 and figure 2 are sketches of P and S types piezo-electric elements. As shown in Figure 1 and Figure 2, piezoelectric element polarized in the perpendicular direction to the electrodes generates P wave and polarized in parallel direction to the electrode produces S wave. A single piezo-element possesses single pattern of vibration. So, measuring both P and S waves simultaneously seek necessity of smart piezo-element enabling to generate or sense both compressional and shear waves and P and S elements are firmly merged having an insulation layer in between two elements for this purpose. The schematic plots of merged PS elements are shown in Figure 3 (a) and (b). During transmitting the signals, both P and S elements are needed to apply the electric voltage at same time. The configuration as shown in Figure 3 (a) allows doing this. In case of receiver, both P and S waves are needed to tap in interpretable manner and meaningfully. That is the reason, the configuration as shown in Figure 3 (b) is adopted in receiver which permits to collect the data of signals individually (P and S wave's data are tapped separately in oscilloscope).

The disk shaped piezo-ceramic elements (P type: diameter = 20mm, thickness = 2mm and S type: diameter = 20mm, thickness = 5mm) were used to form PS type ceramic element. P type and S type elements are merged applying thin layer of epoxy resin. The pictures of P type, S type and merged PS type piezo-ceramic elements are shown in Figure 4. The firmly merged PS type piezo ceramic element is

converted to “Disk Transducer” assembling on metal housing suited to the specimen of 75 mm in diameter and 150 mm in height. The schematic diagram of assembling details and picture of “Disk Transducer” is depicted in Figure 5. The piezo-ceramic element is coated by epoxy resin to protect from harm and water. The Disk Transducer assembled surrounding piezo ceramic elements by thin layer (2 mm x4 mm) of silicon with smooth surface have shown the better performance than rough surfaced Disk Transducer (Suwal et at., 2009). Following to this, the “Disk Transducer” was assembled surrounding piezo-ceramic element by a layer of silicon which permits easy shear motion resulting good performance as compared to rigid one. The piezo-ceramic elements are strongly fixed on metal housing with help of epoxy resin as shown in Figure 5. The Disk Transducer was encapsulated into the top cap and pedestal of the triaxial apparatus.

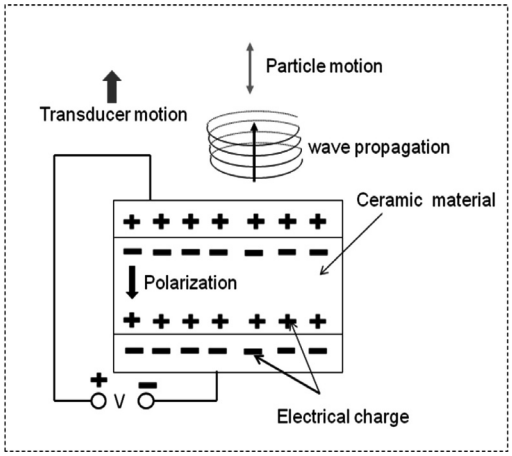

Figure 1. P-type element

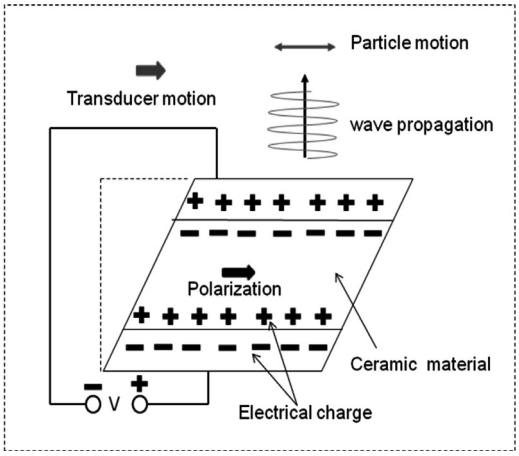

Figure 2. P-type element

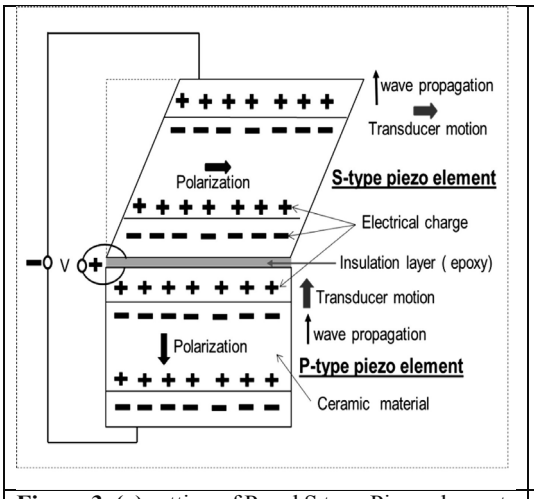

Figure 3. (a) setting of P and S type Piezo elements (Transmitter for simultaneous excitation)

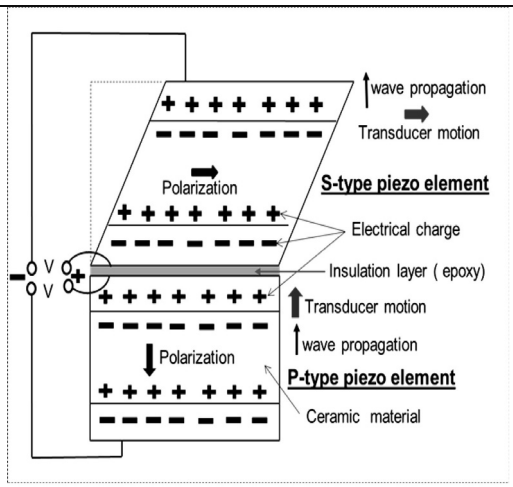

Figure 3. (b) Setting of P and S type Piezo elements (Receiver for simultaneous acquisition)

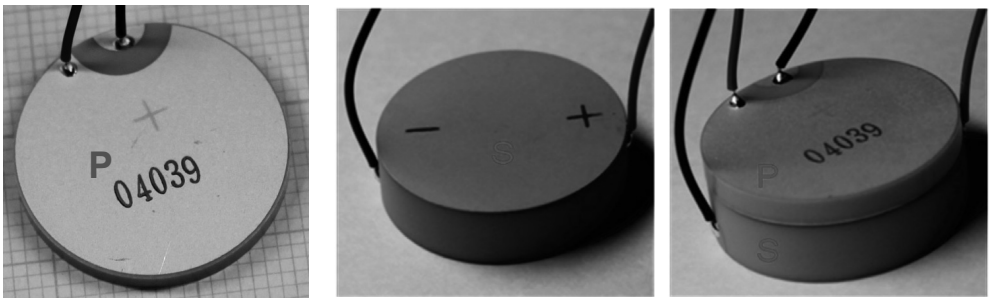

Figure 4. Pictures of Piezo-ceramic element (P type, S type and PS type respectively)

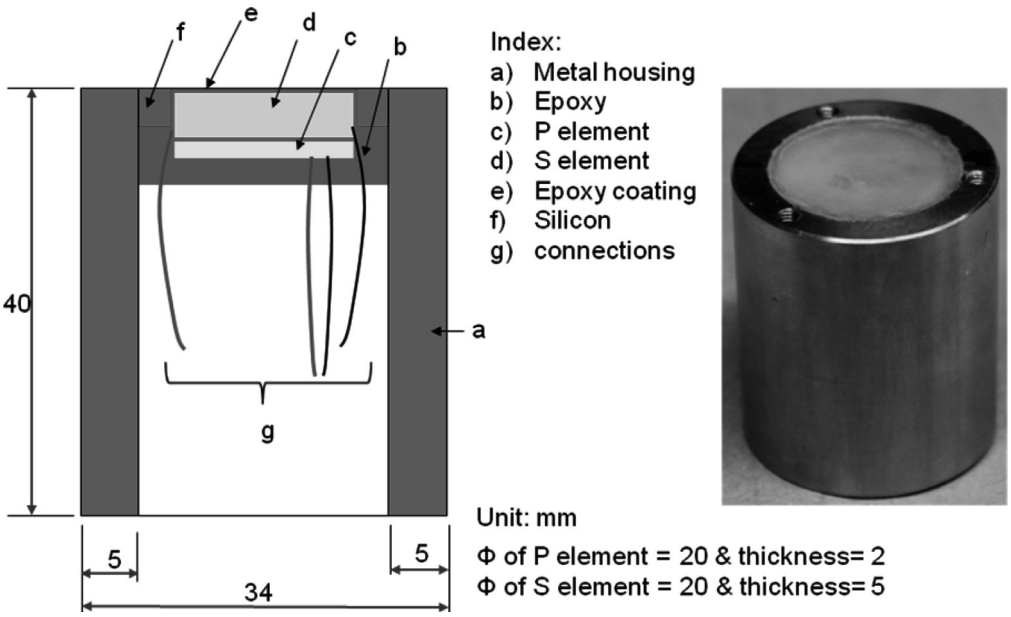

Figure 5. Detailed of the Disk Transducer

PARALLEL ACQUISITION OF ELASTIC WAVES

General assumption:

Disk transducers capsulated into the top cap and pedestal are employed for propagating body waves (compressional and shear waves). Compressional wave is the fastest among the several kinds of waves. For the various soils, it is experienced that the shear wave velocity is nearly half of the compressional wave speed. This is the reason the simultaneous acquisition of compression and shear waves is become possible. When the transmitter is subjected to excitation applying electric voltage in designed pattern through function generator, both elements of Disk Transducer (transmitter) will get excited simultaneously and generate both compressional and shear waves as schematically shown in Figure 6. The compressional and shear waves propagated through the soil (specimen) at different velocities and will reach the compressional wave at first and then followed by the shear wave at the receiver. As shown

in the Figure 3 (b), the receiver is designed enabling to tap both the received compressional and shear waves separately.

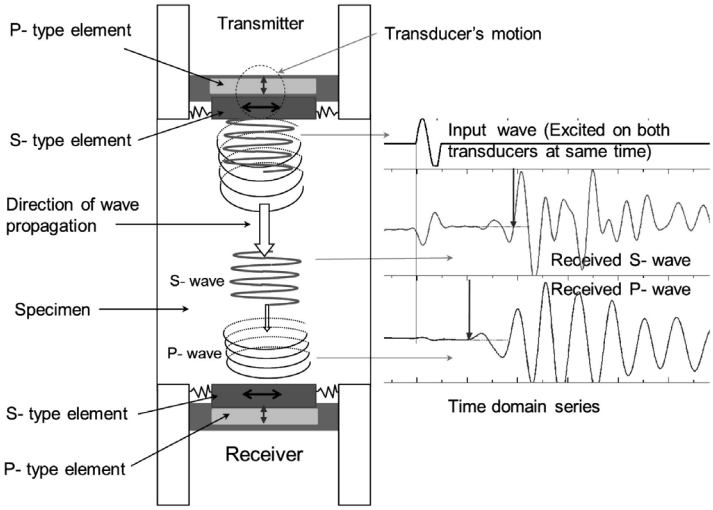

Figure 6 Schematic plot of simultaneous wave propagation technique

Experimental verification of parallel acquisition of elastic waves:

The history of elastic wave measurement technique in geotechnical sector is not itself long and simultaneously measurement of both compressional and shear waves in a single specimen is still rare. The performance of flat surfaced Disk Transducer has been verified with additional merits (Suwal, et al., 2009). To confirm the possibility and eligibility of simultaneously acquired signals, the tests were preliminarily performed on rubber dummy, Toyoura sand. The transmitter transducer was excited generating only compressional wave at first. Then excited generating shear wave and at last excited generating both compressional and shear waves together. The achieved responses (waveforms) on receiver at prior mentioned circumstances are examined and compared. The details are described here;

Test on Rubber dummy:

The rubber dummy as shown in Figure 7 is employed in unconfined condition. The rubber dummy is placed between the top cap and pedestal. To ensure the contact between the transducers (transmitter and receiver) and sample (rubber dummy)), top cap and pedestal were compressed through the loading piston. The value of load 43.3 N was detected by a load cell. A pulse and single sinusoidal signals were excited through transmitter and response on receiver was recorded on multi channels oscilloscope. A typical plot obtained during a pulse excitation is shown in Figure 8. Figure 8 (A) was obtained while P type element in transmitter was subjected to excitation through function generator. The responses on receiver during S wave propagation was shown in Figure 8 (B) and the received signals resulted during both P and S waves propagated in parallel are plotted in Figure 8 (C). Both type of signals (P and S) were recorded in all cases. Observing those signals, it can be seen that P and S wave were detected in Figure 8 (A) and 8 (B) are similar to one seen in Figure 8 (C). This shows that both compressional and shear waves are possible to measure at same time. The compressional and shear signals achieved while exciting individual P type, S type and both P and S types elements are shown in Figure 9. With aid of observed signals shown in Figure 9, the identical responses were noticed either individual piezo-element excitation or both P type and S type element excite together on rubber dummy specimen. Beside the pulse signal, single sinusoidal signals were also propagated and same performances were observed.

Test on Toyoura sand:

Toyoura sand, fine grained sand was used to understand the ability of measuring both compressional and shear waves on a single specimen at same time. Dry Toyoura sand specimen of 75 mm in diameter and 150 mm in height was erected by pluviating through air. A pulse signal and single sinusoidal waves consisting of frequency ranges from 5 to 30 kHz were propagated at isotropic stress state of 50 kPa to 400 kPa. In each stress state, the signals were propagated generating by individual P type and S type element excitation and both P and S type elements excitation together. The received signals through receiver were observed and compared. The typical waveforms obtained on Toyoura sand specimen in isotropic stress state of 50 kPa are shown in Figure 10. These waveforms are achieved while transmitter transducer was excited with a single sinusoidal wave consisting of 20 kHz frequency. Figure 10 (A) was observed while P type element in transmitter was excited, Figure 10 (B) was received while S type element in transmitter was excited and Figure 10 (C) were observed during both P and S elements in transmitter were excited together. The ambiguity about the signals received during single element excitation in transmitter and both elements excitation in transmitter were similar or not is solved comparing the compressional and shear waves obtained in prior mentioned condition in Figure 11 [Upper: compressional wave comparison and lower: shear wave comparison]. The results obtained during single element excitation and both elements excitation are found to be similar and the estimated point of arrival of signal in both cases was found to be identical. The behaviors of elastic wave measurement at higher stress state were examined repeating same processes in several stress states. The results obtained at isotropic stress state of 400 kPa were shown in Figure 12 and 13.

Figure 7. Rubber dummy

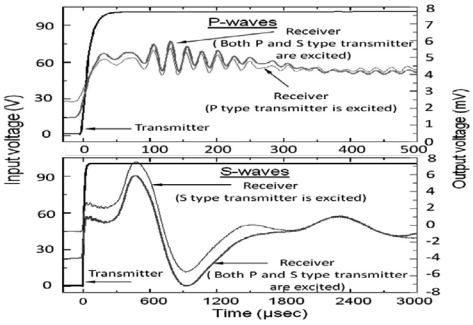

Figure 9. Comparisons of P and S waves obtained on rubber dummy

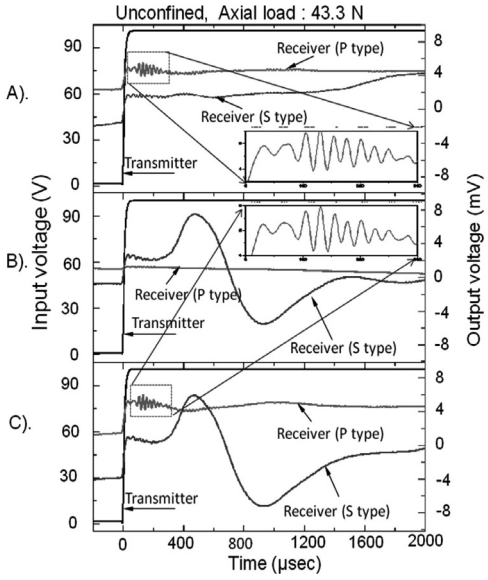

Figure 8. Waveforms obtained on rubber dummy (A) while p-type transmitter excited, (B) while S-type transmitter excited and (C) while P and S type transmitters are excited simultaneously

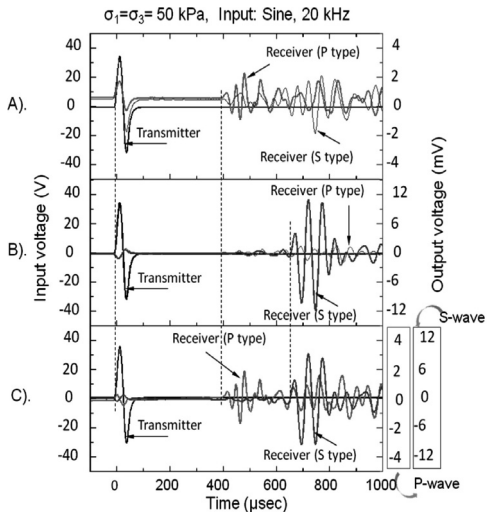

Figure 10. Waveforms obtained on Toyoura sand at 50 kPa isotropic stress state (A) while p-type transmitter excited, (B) while S-type transmitter excited and (C) while P and S type transmitters are excited simultaneously

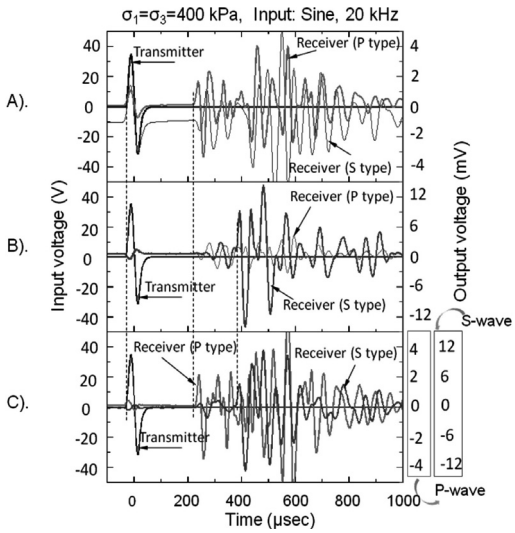

Figure 12. Waveforms obtained on Toyoura sand at 400 kPa isotropic stress state (A) while p-type transmitter excited, (B) while S-type transmitter excited and (C) while P and S type transmitters are excited simultaneously

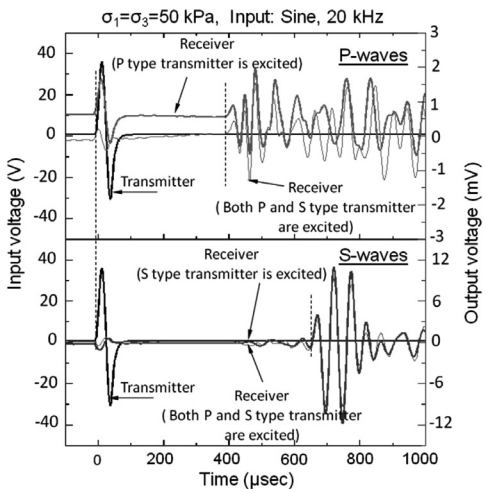

Figure 11. Comparisons of P and S waves obtained on Toyoura sand at 50 kPa

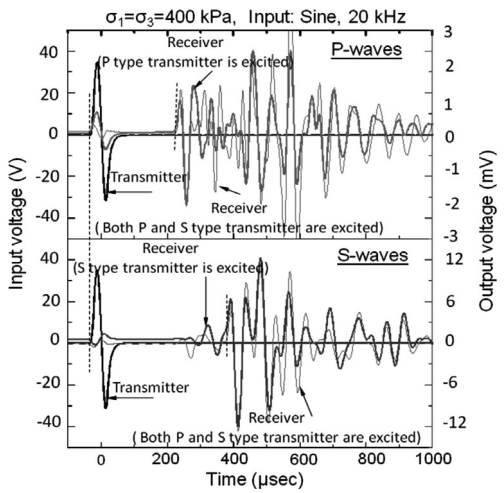

Figure 13. Comparisons of P and S waves obtained on Toyoura sand at 400 kPa

Beside rubber dummy and Toyoura sand, Silica sand and Hime gravel were also tested and the results similar to obtained on Toyoura sand were achieved. Those experimental results shows that the simultaneous measurement of both compressional and shear waves on a single specimen is valid and performance is well.

INTERPRETATION OF SIGNALS IN THIS STUDY

Accurate detection of arrival time of signal is prime factor which affects the dynamically expressed results. Compressional wave is fastest and its detection is not ambiguous amongst the researchers. The determination of arrival time of shear wave tends to be arguable due to the effects of so called near field effects and reflected waves forming complex waveform. Various techniques have been proposed to minimize the uncertainties in the interpretation of the time of arrival (Woods, 1978, Viggaini and Atkinson, 1995, Jovicic et al., 1996; Arulnathan et al. 1998; Blewett et al., 1999; Lee et al, 2005; Kuwano et al., 2008). Cross-correlation method had recommended determining the travel time between two signals in laboratory and field testing (Woods, 1978). Both input and output signals are considered of the same nature in cross-correlation method. This requirement is rarely valid in reality, so results produced by cross correlation method consists of errors. The difference between the computed travel time by cross-correlation method and real travel time had experimentally shown for bender element transducer. The degree of errors (differences) is relevant with the damping ratio, the natural period of the system and the period of the input sinusoidal signal (Viggiani and Atkinson). Viggiani and Atkinson (1995) had advised to employ a sinusoidal signal to minimize the complexities and uncertainties in the interpretation. The same shape signals on input and output signal could be expected using a single sinusoidal signal as the input signal. Jovicic et al. (1996) proposed a single sinusoidal wave as a input signal and adoption of the point of the first inversion as the arrival of shear wave and recommend employing the high frequency signals for reducing the near field effects. Some other researchers tried to apply characteristic points (peaks, troughs) to detect the arrival time of signal. The method of employing continuous sinusoidal waves has been also recently proposed (Blewett et al. 1999; Greening, 2004). The frequency of the input signal is gradually modified until same phase's input and output signals are received. The measurements are repeated for different frequencies (wave lengths). The travel time is determined from the slope of a frequency vs. number of wavelengths line. All the methods discussed above seem to be capable of determining arrival time of signal (travel time) correctly under limited circumstances but equally all appear to have limitations that are not well defined. Experimental and numerical analysis results showed that none of these methods were totally reliable (Arulnathan et al., 1998; TC29 round robin test). The compressional waves are evaluated as the first deflection of the signal on time domain is the arrival of the compressional waves. Figure 14 shows the typical compression waveform obtained in this study. The travel time are dealt considering the time gap between the starting of the input signal and the starting of output signal. The travel time of propagated shear wave is determined as recommended by Jovocic (1996). The zero baseline correction is imposed to minimize the effect of the near field. The typical waveform indicating the point of arriving of the received shear wave is shown in Figure 15.

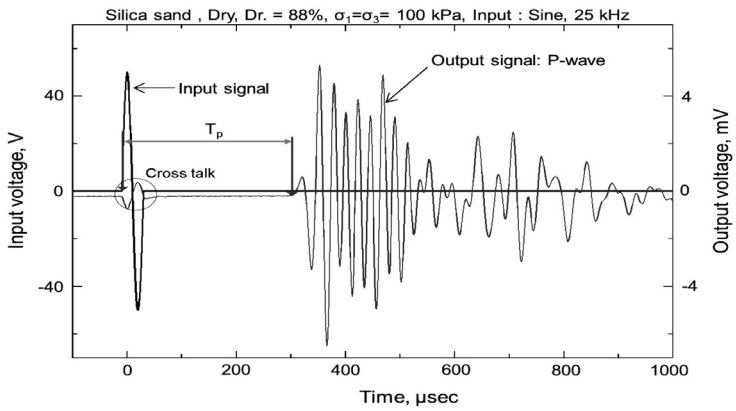

Figure 14. Travel time considered in P wave propagation

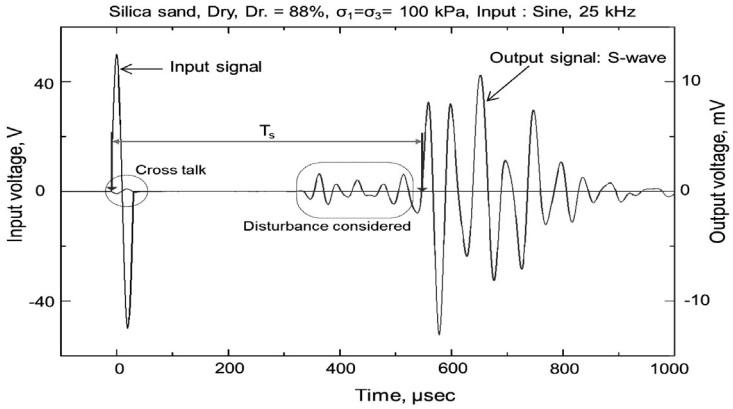

Figure 15. Travel time considered in S wave propagation

MEASUREMENT ON GRANULAR MATERIALS

Material used:

Toyoura sand is fine-grained, uniformly graded sand, originated from Toyoura Beach area of Yamaguchi prefecture, Japan. It looks light yellowish- brown in color and well sorted. It is derived from the siliceous rocks and shale. So it contains well rounded quartz particles. Silica sand is one of the popular varieties of sand in the world. Silica sand is produced by degradation of quartz. The quartz crystals are broken down into small grains as Silica sand. The grain size of Silica sand varies from fine to coarse. In this study, Silica sand (No. 5) having mean diameter, D_{50}, of 0.45mm was used. Hime gravel is poorly sorted, and the grains are angular. It was taken from Hime River, Otari, Kitaazumi, Nagano prefecture, Japan. It is derived from sandstone, chart, granite, shale, quart etc. The photograph of the used materials is shown in Figure 16. Physical properties including specific gravity, maximum and minimum void ratio and mean diameter are shown in Table 1 and gradation curves is given in Figure 17.

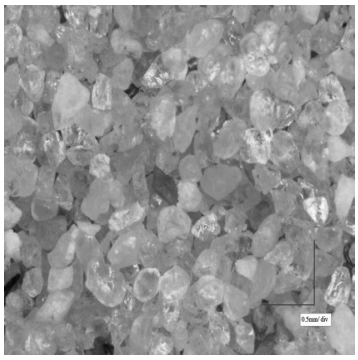

Figure 16. (a) Toyoura sand

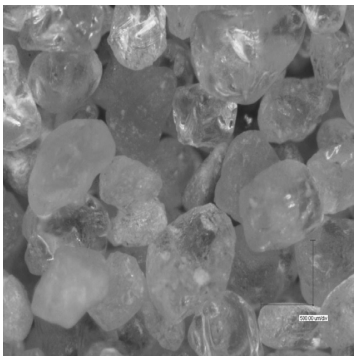

Figure 16. (b) Silica sand

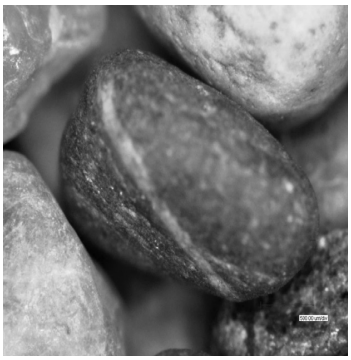

Figure 16. (c) Hime gravel

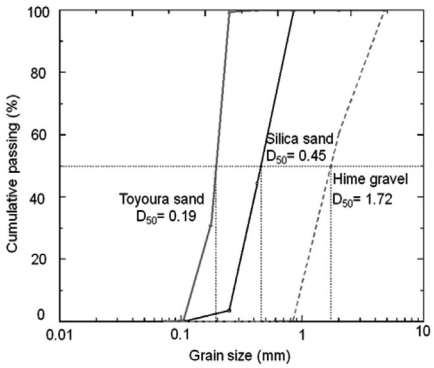

Figure 17. Particle size distribution chart of used materials

Table 2: Physical and mechanical properties of tested materials

Physical and mechanical Properties	Toyoura sand	Silica sand	Hime gravel
Specific gravity, G_s	2.62	2.64	2.65
Maximum void ratio, e_{max}	0.946	0.787	0.709
Minimum void ratio, e_{min}	0.637	0.538	0.480
Mean Diameter, D_{50} (mm)	0.19	0.45	1.72

Apparatus:

The triaxial apparatus sophisticating with various transducers/sensors for strains and elastic wave measurement was employed in this study. Broadly they are categorized in three groups as;

Triaxial compression testing machine: Small size, gear driven and strain controlled triaxial apparatus was used for conducting tests. The axial loading system consists of an AC servomotor and a reduction gear system, electro-magnetic clutches and brakes. Experiments were performed controlling stress and strain precisely by closed loop feedback system. The analog to digital and digital to analog converters were used in closed loop feedback system to control the experiments. The photograph of the employed triaxial apparatus is shown in Figure 18.

Transducers for strain measurement: Axial (vertical) and lateral (radial) strains are monitored by Local Deformation Transducer (LDT) and Clip gauges. LDT is the strain gauge based transducer developed in laboratory following to Goto et al., 1991, which can measure local strain in higher accuracy and free from bedding errors. A pair of LDTs was fixed on the cylindrical specimen in each cases enabling to measure axial deformation. Clip gauges were used to measure radial strain variations on specimen during the experiments. Commercially available clack gauges were modified suited to the specimen of 75mm in diameter and 150 mm in height. Three clip gauges are fixed on the specimen and the average result was analyzed. The photographs of LDT and clip gauge are shown in Figure 19 and Figure 20. The scheme of LDTs and clip gauges layout including wave measurement transducer is shown in Figure 21.

Wave measurement equipment: Beside transducers, wave measurement system consists of chain composed instruments. It includes three electrical devices; (1) Signal generating device (function generator), (2) An amplifier and (3) Signal acquiring device (oscilloscope).

Signal for propagating wave was generated by a digital automatic function generator. It can produce a maximum peak to peak voltage of 10 V and is capable of producing twelve kinds of different waveforms at frequency ranges of 0.001Hz to 25MHz. A function generator is only capable to generate the signal of maximum peak to peak voltage of 10 V. Signals of higher voltage were fed in this study. An amplifier was used to amplify the input signal generated by the function generator before feeding it into the transducer. The multi channels oscilloscope was used to record and display waveforms of the transmitted and received signals. The pictures of the oscilloscope including the function generator and the amplifier are shown Figure 21.

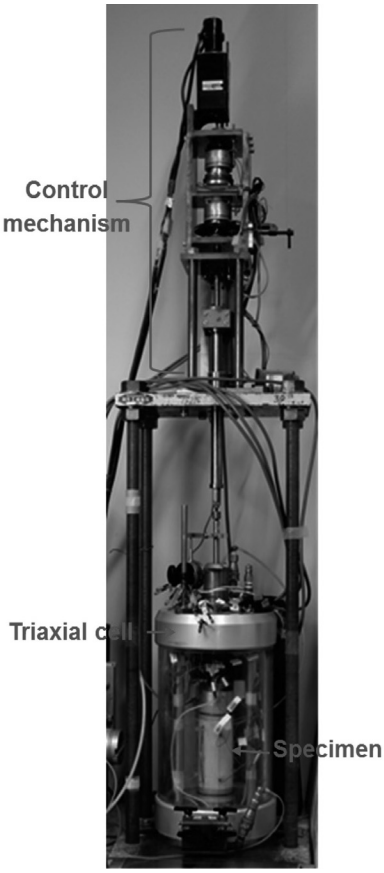

Figure 18. Triaxial apparatus

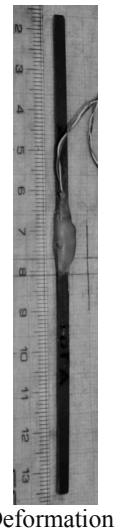

Figure 19. Local Deformation Transducer (LDT)

Figure 20. Clip gauge

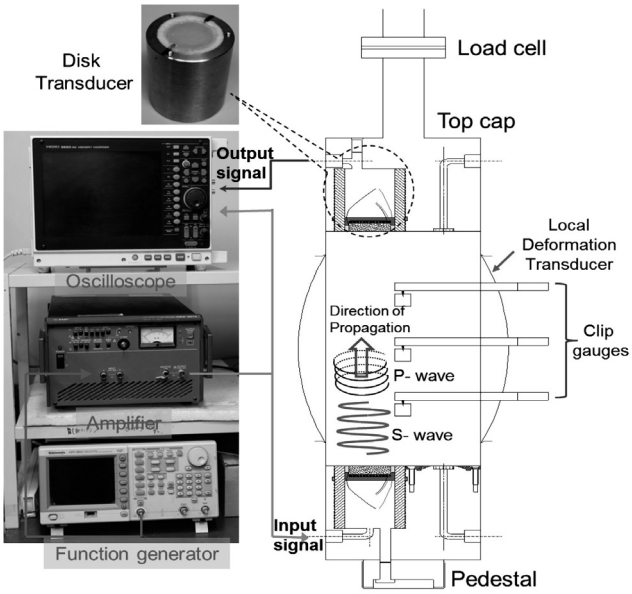

Figure 21. Layout of transducers and elastic wave measurement technique

Methodology:

Specimen preparation: The tested materials were granular so the pluviation technique was adopted for specimen preparation. Approximately homogeneous densities were maintained controlling pouring height. While pouring the materials, the vertical distance between the top surface of the sand and the tip of the funnel opening was maintained constant and the pouring direction was changed from clockwise to anti clockwise regularly .The specimens of 75mm in diameter and height 150 mm were prepared at stress state of 25kPa in all cases.

Loading sequences

Isotropic stress path: As prior mentioned, the samples were made at an isotropic stress state of 25 kPa. Then, the stress level was increased to 50, 100, 200 and 400 kPa respectively. The stress level was increased isotropically till 50 kPa at first and the creep stage was maintained for a while (10 minutes) to dissipate the stress thoroughly. Then 11 cyclic loadings with peak to peak strain amplitude of 0.001% were applied in vertical direction. The strain rate of cyclic loadings was maintained at 0.023mm/min. Again creep stage for elastic wave measurements was maintained. These procedures were repeated on each stress level. Dynamic measurement (elastic wave measurement) was conducted after cycling loading in creep stage.

Anisotropic stress path: The over consolidated specimen was subjected into the anisotropic stress path. The stress level is decreased until 25 kPa stress state maintaining isotropic stress state. The specimen was enforced into the anisotropic stress states controlling both axial and radial stresses (σ_1 and σ_3).The radial stress (σ_3) was kept constantly 25 kPa and axial stress (σ_1) is raised to 50 kPa, 75 kPa, 100 kPa, 125 kPa and 150 kPa. 11 cyclic loadings with peak to peak strain amplitude of 0.001% were applied in vertical direction. The strain rate of cyclic loadings was maintained as similar to isotropic stress cases. Creep stage for elastic wave measurements was maintained. These procedures were repeated on each stress states. The schematic diagram of stress path is shown in Figure 22.

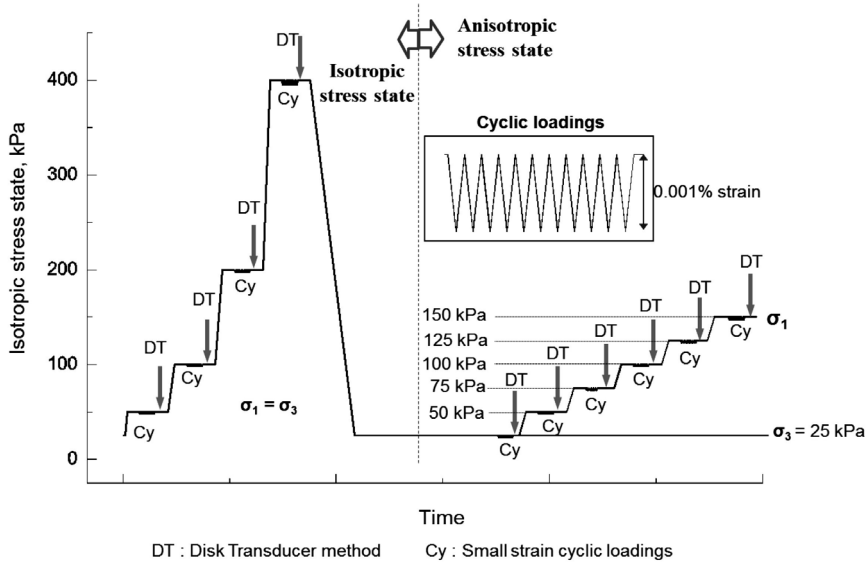

Figure 22. Schematic of loading sequences

Data acquisition and analysis:

Quality of acquired data governs the fineness of the experimental works. LDTs and Clip gauges were adopted for axial and radial strains. Both strain increments were measured continuously throughout the experiment. Axial and radial strains were evaluated as;

$$\text{Axial strain, } \varepsilon_a = -\int_{H_o}^{H} \frac{dH}{H} = -\ln(\frac{H}{H_o}) \quad (1)$$

$$\text{Radial strain, } \varepsilon_r = -\int_{R_o}^{R} \frac{dR}{R} = -\ln(\frac{R}{R_o}) \quad (2)$$

Negative sign in Eqn. (1) and (2) indicates compression is considered as positive.

Poisson's ratio and stiffness are determined based on stress strain behaviors observed during small strain cyclic loading along the vertical direction (axial direction). The elastic parameters were directly calculated as;

$$\text{Young's Modulus, } E = \frac{\delta\sigma}{\delta\varepsilon_a} \quad (3)$$

$$\text{Poisson's ratio, } \nu = -\frac{\delta\varepsilon_r}{\delta\varepsilon_a} \quad (4)$$

Where,
$\delta\varepsilon_r$ = strain variation in radial direction
$\delta\varepsilon_a$ = strain variation in axial direction
$\delta\sigma$ = stress variation in axial direction
The velocity of waves were determined by,

$$\text{Compressional wave velocity, } V_p = \frac{H}{T_p}$$

$$\text{Shear wave velocity, } V_s = \frac{H}{T_s} \quad (5)$$

Where,
H = the height of specimen (Distance between transmitter and receiver)
T_p = time period to propagate the compressional wave from transmitter to receiver.
T_s = time period to propagate the shear wave from transmitter to receiver.

Shear modulus (G), constrained modulus (M) and young's modulus (E) were found out as;

$$\text{Shear modulus, } G = \rho * V_s^2 \quad (6)$$

$$\text{Constrained modulus, } M = \rho * V_p^2 \quad (7)$$

$$\text{Young's modulus, } E = \frac{M(1-2\nu)(1+\nu)}{(1-\nu)} \quad (8)$$

Based on an anisotropic elasticity modeling proposed by Tatsuoka et al. (1999) considering both the inherent and stress state induced anisotropy, shear and young's modulus is related as;

$$G = \frac{E}{2(1+\nu)} \frac{2(1-\nu)}{1 + aR^n - 2\sqrt{a}.R^{n/2}.\nu} \tag{9}$$

Where,

a = the coefficient on the degree of inherent anisotropy. It is set 1 neglecting the possible effect of inherent anisotropy in this study.

R = the stress ratio ($R = \sigma_v/\sigma_h$)

n = the stress state dependency coefficient

When isotropic stress condition is considered (R= 1), the equation (9) is changed to;

$$G = \frac{E}{2(1+\nu)} \tag{10}$$

The densities of specimens were different in experiments, so the void ratio function proposed by Hardin and Richart (1963) was used to eliminate the effects of various densities (void ratio) of specimens in both isotropic and anisotropic stress conditions.

$$\text{Void ratio function,} \quad f(e) = \frac{(2.17-e)^2}{(1+e)} \tag{11}$$

Where, e = void ratio

TEST RESULTS AND DISCUSSIONS

Test cases

Totally 14 test results, 5/5 tests on Toyoura sand / Silica sand and 4 tests on Hime gravel are included. The information of tests is listed in Table 4. Three sorts of materials were investigated. Toyoura sand represents the fine grain material, Silica sand represents the medium grain material and Hime gravel stands for the coarse grain material.

Table 4: List of experiments

Test no.	Material	Stress phases	Transducer used	Specimen condition	Relative density (%)	Input frequency range (kHz)
T-1	Toyoura sand	Isotropic	DT	Dry	77	10.0 – 40.0
T-2	Toyoura sand	Isotropic	DT	Dry	58	10.0 – 40.0
T-3	Toyoura sand	Isotropic	DT	Dry	83	10.0 – 40.0
T-4	Toyoura sand	Isotropic/anisotropic	DT	Dry	99	10.0 – 40.0
T-5	Toyoura sand	Isotropic/anisotropic	DT	Dry	68	10.0 – 40.0
S-1	Silica sand	Isotropic	DT	Dry	97	10.0 – 40.0
S-2	Silica sand	Isotropic	DT	Dry	92	10.0 – 40.0
S-3	Silica sand	Isotropic/anisotropic	DT	Dry	88	10.0 – 40.0
S-4	Silica sand	Isotropic/anisotropic	DT	Dry	75	10.0 – 40.0
S-5	Silica sand	Isotropic/anisotropic	DT	Dry	62	10.0 – 40.0
H-1	Hime gravel	Isotropic	DT	Dry	84	5.0 – 35.0
H-2	Hime gravel	Isotropic	DT	Dry	70	5.0 – 35.0
H-3	Hime gravel	Isotropic/anisotropic	DT	Dry	75	5.0 – 35.0
H-4	Hime gravel	Isotropic/anisotropic	DT	Dry	94	5.0 – 35.0

Elastic parameters in isotropic stress states

Evaluation of small strain stiffness: Eleven cyclic loadings with peak to peak strain amplitude 0.001% was executed at each stress state. Young's modulus at each stress level was calculated employing Equation (3). The typical stress-strain variations obtained on Toyoura sand specimen (T-5) at isotropic stress state of 50 kPa is shown in Figure 23. This plot was derived from the stress and strain variation data of 10th cycle of cyclic loadings. The average value of 5th and 10th cycles is considered as representative value of Young's modulus in regarding stress states.

As mentioned in stress path, the signals were propagated in each stress states, the typical waveforms obtained on 50 kPa to 400 kPa isotropic stress states on Toyoura sand specimen are shown in Figure 29. Compressional and shear waves are separately shown. Those signals were achieved exciting single sinusoidal wave of 25 kHz through transducer in top cap. The adopted point of arriving signal is shown in corresponding plot. Travelling time was calculated in each case and the velocities were calculated following to Equation (5). Similarly, the waveforms of input and output signals obtained on Silica sand and Hime gravel specimens at several isotropic stress states are calculated.

Statically derived Young's moduli by Equation (3) were converted to the shear moduli using Equation (10) in isotropic stress states. The Poisson's ratio determined by static method was employed. Using Equation (6), shear moduli by Disk Transducer method were directly computed. The shear moduli obtained on numerous specimens were normalized by Eqn. (11) to nullify the effects of void ratios. The normalized shear moduli obtained on Toyoura sand were plotted against the stress state in Figure 25. The filled symbols are associated with the results obtained by static method and open symbols are representing the results obtained by Disk Transducer method. The results derived by both static and Disk Transducer method are found to be in same ranges. Similarly, the normalized shear moduli obtained on Silica sand and Hime gravel specimens are presented in Figures 26 and 27. The meanings of the symbols are similar to Figure 25. In those plots, the equivalent stiffness by both static and Disk transducer methods could be seen.

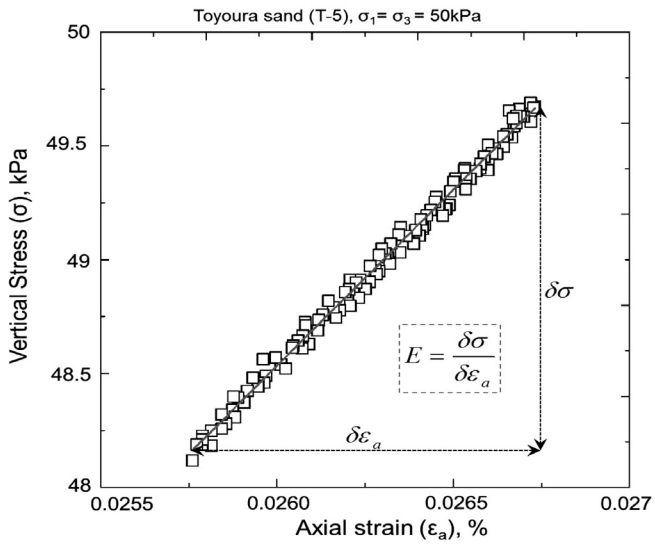

Figure 23. Typical stress-strain relationship of cyclic loading

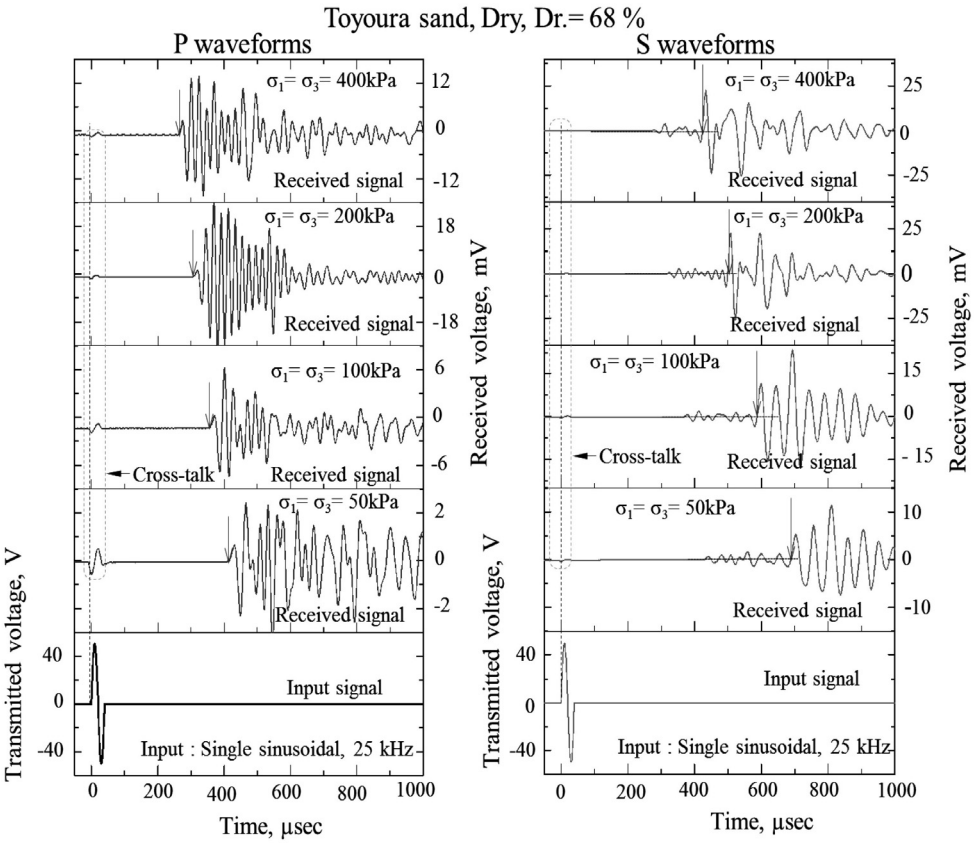

Figure 24. Waveforms obtained on Toyoura sand at isotropic stress state

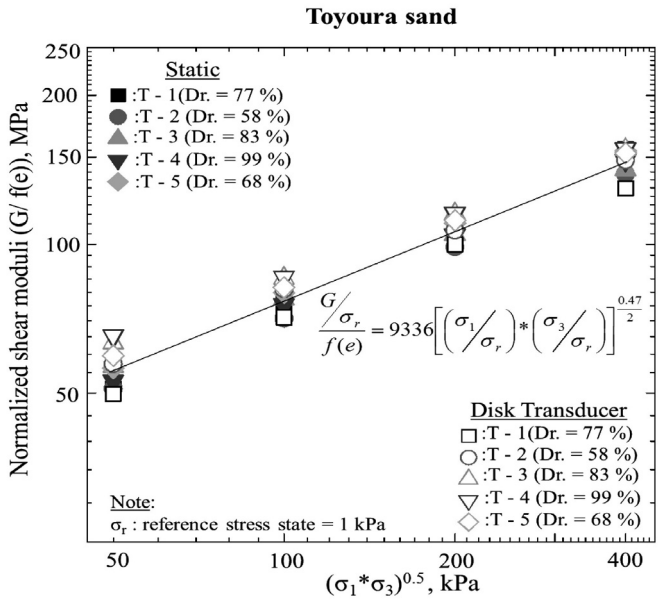

Figure 25. Stiffness obtained on Toyoura sand at isotropic stress state

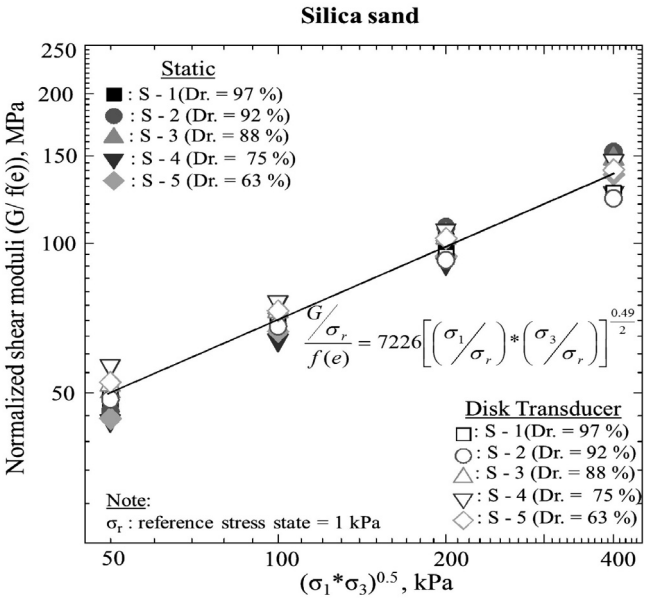

Figure 26. Stiffness obtained on Silica sand at isotropic stress state

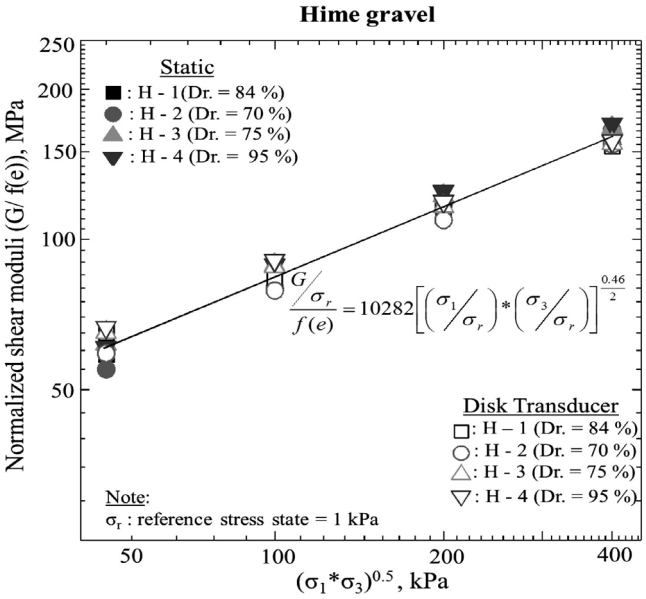

Figure 27. Stiffness obtained on Hime gravel at isotropic stress state

Elastic parameters in anisotropic stress states

Evaluation of small strain stiffness: As shown in stress path, anisotropic stress state was created increasing axial stress step by step maintaining 25 kPa radial stress. In each step, the axial stress was increased by 25 kPa. Eleven cyclic loadings with peak to peak strain amplitude 0.001% were executed at each stress level. Young's modulus was calculated employing Equation (3) as isotropic stress state. Then shear modulus was computed based on an anisotropic elasticity modeling considering stress state

induced anisotropy. The coefficient of the degree of inherent anisotropy was set equal to **1**, neglecting inherent anisotropy in this study.

The typical waveforms obtained on Toyoura sand specimen at several anisotropic stress states are shown in Figure 28. Those signals were achieved exciting single sinusoidal wave of 25 kHz through transducer in top cap on experiment T-4. The arrival points of signal in time domain series are shown in corresponding plot. The travel time is found to be the shorter at the higher axial stresses in P waveforms. But the travel time is found the shortest at certain axial stress state and then tending to be larger with increasing axial stresses in S waveforms. This phenomenon can be clearly seen in Figure 28. Similarly, the waveforms of input and output signals obtained on Silica sand and Hime gravel specimens at various anisotropic stress states are evaluated. Velocities of propagating compressional and shear (P and S) waves were determined following to Equation (5). Then the stiffness moduli were computed by Equations (6), (7) and (8).

Statically derived shear moduli and shear moduli by Disk transducer method were normalized by equation (11). The normalized shear moduli obtained on Toyoura sand were plotted against the stress state in Figure 29. The square and triangle are used to express the statically calculated results and circles for dynamically derived results. While converting statically derived young's moduli into the shear moduli, the Poisson's ratios determined by both statically and dynamically are employed and the obtained results are presented in the plot. Shear moduli were found to be increased smoothly upto axial stress 75 kPa (σ_1/σ_3 = 3) and then tending to be decreased. Similarly, the normalized shear moduli obtained on Silica sand and Hime gravel specimens are presented in Figures 30 and 31.

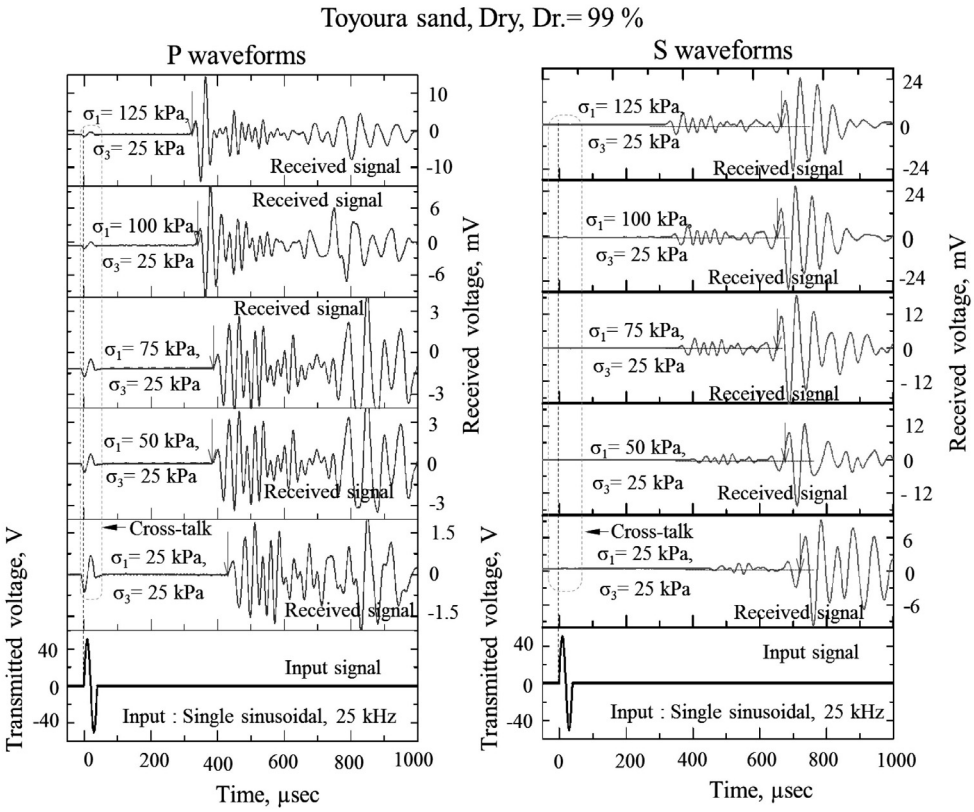

Figure 28. Waveforms obtained on Toyoura sand at anisotropic stress state

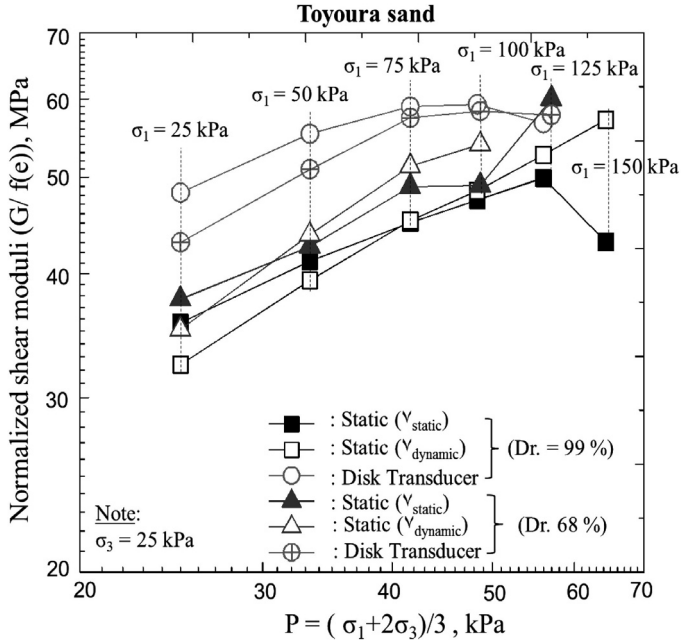

Figure 29. Stiffness obtained on Toyoura sand at anisotropic stress state

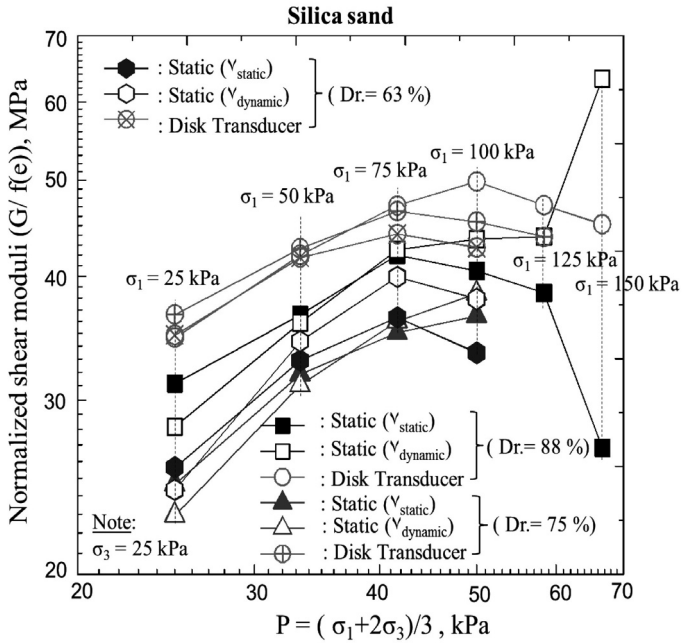

Figure 30. Stiffness obtained on Silica sand at anisotropic stress state

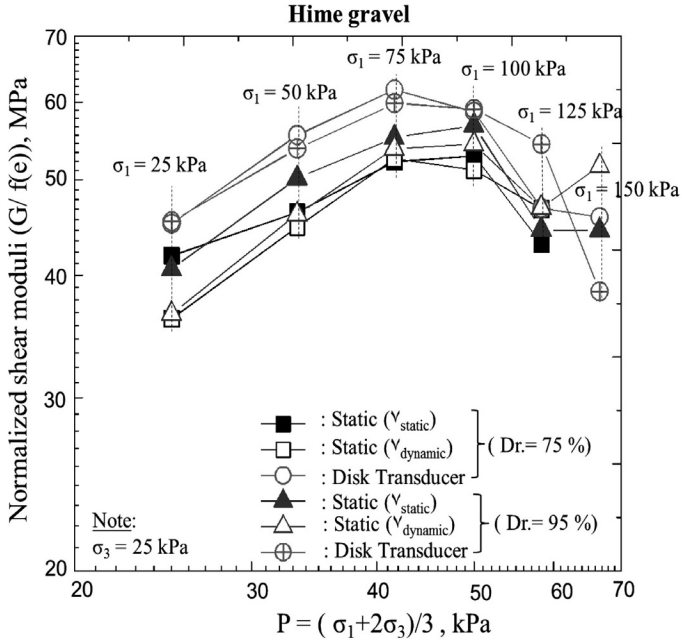

Figure 31. Stiffness obtained on Hime gravel at anisotropic stress state

CONCLUSIONS

The compressional and shear waves are successfully measured in parallel on Toyoura sand, Silica sand and Hime gravel specimens. Elastic parameters of those materials were investigated by both statically and dynamically in isotropic and anisotropic stress states. Based on the achieved results, the followings are concluded:

- The compressional and shear waves were successfully propagated simultaneously in triaxial specimens. The Disk Transducer method was introduced for measuring both the compressional and the shear waves in a single specimen at the same stress state simultaneously. The waveforms of individually propagated compressional and shear waves and simultaneously achieved compressional and shear waves were compared and performance was found to be equivalent.
- The elastic properties; small strain stiffness of three sorts of granular materials, Toyoura sand, Silica sand and Hime gravel were evaluated by both statically applying small strain cyclic loadings and dynamically employing Disk Transducer method in isotropic and anisotropic stress states.
- In isotropic stress states, the equivalent shear moduli were achieved by both static and Disk Transducer method. In anisotropic stress states, the shear moduli obtained by Disk Transducer method were found to be slightly higher than one obtained by applying small strain cyclic loadings

REFERENCES

Ackerly, S. K., Hellings, J. E. and Jardine, R. J. (1987): Discussion on a new device for measuring local axial strain strains on triaxial specimens, Geotechnique, 37(3), 413-417

Arulnathan, R., Boulanger, R. W., and Riemer, M. F. (1998): Analysis of Bender Element Tests, *Geotechnical Testing Journal*, 21(2), 120-131.

Blewett, J., Blewtt, I. J and woodward, P. K. (1999): Measurement of shear-wave velocity using phase sensitive detection technique, *Canadian Geotechinical Journal.* 36(5), 934-939.

Brignoli, E. G. M., and Stokoe, K. H., II. (1996): Measurement of shear waves in Laboratory Specimens by Means of Piezoelectric Transducers, *Geotechnical Testing Journal*, 19(4), 384-397.

Burland, J. B. (1989): Ninth Laurits Bjerrum Memorial Lecture: Small is Beautiful-The Stiffness of Soils at Small Strain", *Canadian Geotechnical Journal*, 26(4), 499-516.

Burland, J.B. and Symes, M. (1982): A simple axial displacement gauge for use in triaxial apparatus, *Geotechnique*, 32(1), 62-65.

Di Benedetto, H., and Tatsuoka, F., (1997): Small strain behavior of geomaterials: Modelling of strain rate effects", *Soils and Foundations*, 37(2), 127-138.

Goto, S., Tatsuaka, F., Shibuya, S., Kim, Y-S., and Sato, T. (1991): A simple Gauge for local small strain Measurements in the laboratory, *Soils and Foundations*, 31(1), 169-180.

Greening, P. D. and Nash, D. F. T. (2004): Frequency domain determination of Go using bender elements, *Geotechnical Testing Journal*, 27(3), 288-294.

Hicher, P. Y. (1996): Elastic properties of soils, *Journal of Geotechnical Engineering*, 122(8), 641-648

Hird, C. C. and Yung, P.C.Y. (1989): The use of proximity transducers for local strain measurements in triaxial tests, *Geotechnical Testing journal*, 12(4), 292-296.

Jamiolkowski, M., Lancellotta, R. and Lo Presti, D.C. F. (1995): Remarks on the stiffness at small strains of six Italian clays, *Pre-failure Deformation of Geomaterials* (edited by: Shibuya S. et al.) Balkema, 817-836.

Jovicic, V., Coop, M. R., and Simic, M. (1996): Objective Criteria for Determining Gmax from Bender Element Tests, *Geotechnique*, 46(22), 357-362.

Kuwano, R., Connolly, T. M. and Kuwano, J. (1999): Shear stiffness Anisotropy Measured by multi-directional Bender element Transducers, *Proceedings of Second International Symposium on Prefailure Deformation Characteristics of Geomaterials*, Torino, Jamiolkowsky, Lancellotta, and Lo Presti, EDs., Balkema, Vol. 1, pp.: 205-212.

Kuwano, R., Wicaksono, R.I and Mulmi, S. (2008): Small strain stiffness of coarse granular materials measured by wave propagation, *Proc. of 4th international symposium on deformation characteristics of geomaterials*, IS-Atlanta 2008, Vol.2, 749-756.

Lawrence, F. V., (1963): Propagation of Ultrasonic Waves Through Sand, Research report R63-8, Massachusetts Institute of Technology, Cambridge, MA, March

Lawrence, F. V., (1965): Ultrasonic Shear Wave Velocity in Sand and Clay, Research report R65-05, Soil Publication No. 175, Massachusetts Institute of Technology, Cambridge, MA, January

Lee, J. S. and Sanatamarina, J. C. (2005): Bender Elements: Performance and Signal Interpretation, *Journal of Geotechnical and Geo-environmental Engineering*, 131(9), 1063-1070.

Lee, C., Truong, Q.H. and Lee, J. S. (2010): Cementation and bond degradation of rubber-sand mixtures, *Canadian Geotechnical Journal*, 47, 763-774.

Lo Presti, D.,Pallara, O.,Lancelotta, R.,Amandi, M. and Maniscalco,R. (1993): Monotonic and cyclic loading behavior of two sands at small strains, *Geotechnical Testing journal*, 16, (4), 409-424.

Mulmi, S., (2008): Small-strain Stiffness Measurement of Geomaterials byElastic Waves, *Master Thesis*, Department of Civil Engineering, the University of Tokyo, Japan.

Shirley, D. J., and Hampton, L. D. (1978): Shear-wave Measurements in Laboratory sediments, *Journal of Acoustical Society of America*, 63(2)

Suwal,L..P., Kuwano,R., Ebizuka,H. and Sato,T. (2009): Performance of Plate Transducer - Transducer for Dynamic Measurement in Laboratory Specimens, *Proc. of 11th International Summer Symposium, International Activities Committee, JSCE*, 113-116.

Tatsuoka, F. and Kohata, Y (1995): stiffness of Hard soils and soft rocks in Engineering applications, *keynote Lecture, Proceedings of International Symposium Pre-failure Deformation of Geomaterials* (Shibuya et al., eds), Balkema, 2, 947-1063.

Tatsuoka, F. and Shibuya, S. (1992): Deformation Characteristics of Soils and Rocks from Field and Laboratory Tests, *Proceedings of 9th Asian Regional Conference of SMFE*, Bangkok, 2, 101-170.

Viggiani, G. and Atkinson, J. H. (1995): Interpretation of Bender Element Tests, *Geotechnique,* 45(1), 149-154.

Woods, R. D., (1991): Field and Laboratory Determination of Soil Properties at Low and High Strains, *Proceedings of second International Conference on Recent Advances in Geotechnical Earthquake Engineering and Soil Dynamics*, pp. 1727-1741.

Yamashita, S., Kawaghchi, T., Nakata, Y., Mikami, T., Fujiwara, T. and Shibuya, S. **(TC 29, round robin test),** (2009): Interpretation of international parallel test on the measurement of Gmax using bender elements, Soils and Foundations, 49, 631-650.